

Letter

External magnetic field-assisted polarization-dependent optical bistability and multistability in a degenerate two-level EIT medium

Anh Nguyen Tuan¹, Hien Nguyen Thi Thu^{1,2}, Thanh Thai Doan¹, Doai Le Van², Khoa Dinh Xuan², Bang Nguyen Huy², Nga Luong Thi Yen^{2,*} and Dong Hoang Minh^{1,*} 

¹ Ho Chi Minh City University of Food Industry, Ho Chi Minh City, Vietnam

² Vinh University, 182 Le Duan Street, Vinh City, Vietnam

E-mail: ngalty@vinhuni.edu.vn and dong.gtvmt@gmail.com

Received 5 October 2022

Accepted for publication 28 December 2022

Published 20 January 2023



Abstract

In this paper, a novel degenerate two-level model is proposed to study the behavior of optical bistability (OB) and optical multistability (OM) under the effect of the magnetic field and relative phase. We show that the behavior of the OB can appear in the resonant regime by changing the strength of the external magnetic field. Especially, the result has shown that it is possible to easily convert between OB and OM by adjusting the strength of the external magnetic field or coupling field in the presence of the relative phase. In addition, the influence of the probe detuning and the atomic cooperation parameter on the OB behavior have also been considered. The studied results may be helpful for optical communication applications in optical switching processing and optimization.

Keywords: degenerate atomic medium, optical switching, optical bistability and multistability, electromagnetically induced transparency, polarization

(Some figures may appear in colour only in the online journal)

1. Introduction

Optical bistability (OB) is an engaging topic and has always attracted the attention of scientists because of its potential applications in all-optical switching, optical transistors, and quantum information [1]. Almost of the research on OB have been conducted in two-level atomic systems both theoretically and experimentally [2, 3]. However, due to the passive optic nature of the two-level medium, the behavior of the bistability curves of the received signal beam at the output

is controlled by the input beam itself. Recently, there has been a significant trend in the research interest of scientists to multilevel atomic systems related to quantum coherence phenomena [4]. Especially with the advent of the electromagnetically induced transparency (EIT) effect [5, 6] has created many new phenomena such as lasing without population inversion [7], enhancement of Kerr nonlinearity [8–11], ultra-slow light propagation [12–17], OB and all-optical switching [18–23]. Therefore, OB and optical multistability (OM) behaviors in multilevel systems have also been studied theoretically and experimentally [24–38]. The advantage is that it is possible to create a large nonlinear medium inside an optical cavity at low light intensity compared to a two-level system

* Authors to whom any correspondence should be addressed.

[24]. Furthermore, external coupling fields can change the optical characteristics of the multilevel system [25]. In this case, the underlying mechanisms for tailoring the properties of the medium are quantum interference and coherence effects. From these antecedent studies, Harshawadhan and Agarwal [26] proved that the threshold intensity of the OB is considerably attenuated by quantum interference and coherence effects. In addition, the great width of the OB can be reached in a three-level atomic model via the enhancement of the initial coherence [27].

Besides, the behavior of OB in a three-level Rb atomic medium was also experimentally demonstrated by Joshi *et al* [28, 29]. These works also found that it is possible to use the intensity of the coupling laser field or the frequency detuning to control the properties of OB. Also, the behavior of single OB, double OB, and optical tristability in a three-level V-type atomic system without considering coherent control by an incoherent pump field, microwave field, or spontaneously generated coherence (SGC) can be obtained [30]. They clarified the physical principles of various bistable and tristable states, particularly switching from absorptive to dispersive characteristics. Other proposals also found that the threshold and the hysteresis loop of OB can be dramatically modified under the quantum interference effect [31], the relative phase [32], and spontaneously generated emission [33]. Furthermore, the properties of OB and OM via the incoherent pumping and magnetic field have also been studied [34–38]. The results of these studies have shown the possibility of controlling the behavior of the OB and conversion from OB to OM and vice versa by relative phase.

In this paper, we use the degenerate two-level EIT medium to investigate the properties of OB and OM based on the magnetic field's strength variation and polarization-dependent phase difference ϕ . The bistability behavior is manipulated by using the external magnetic field, control field, probe detuning, relative phase, and atomic cooperating parameter. Moreover, in the presence of a relative phase, we can convert between OB and OM by changing the strength of the magnetic field. The results obtained are useful for optical switching and storage applications. Furthermore, the model can be experimentally generated easily because of using a single laser source for both probing beam and coupling beam in different frequency regimes.

2. Model and basic equations

We consider a degenerate two-level atomic system under the effect of the probe and coupling laser fields, as depicted in figure 1(a). Here, the transition $|2\rangle \leftrightarrow |1\rangle$ coupled by the σ^- polarized probe field E_p has the Rabi frequency $\Omega_p = \mu_{21}E_p/2\hbar$. At the same time, the transition $|2\rangle \leftrightarrow |3\rangle$ is coupled with the σ^+ polarized strong coupling field E_c has the Rabi frequency $\Omega_c = \mu_{23}E_c/2\hbar$. In this model, the probe field is traveling in the direction parallel to both the polarization of the coupling field and the direction of the applied longitudinal magnetic field B , which is used to remove the degeneracy among the ground-state sublevels $|1\rangle$ ($m_F = -1$) and

$|3\rangle$ ($m_F = +1$). The Zeeman shift of the levels $|1\rangle$ and $|3\rangle$ is given by $\Delta_B = \mu_B m_F g_F B/\hbar$, where μ_B and g_F are the Bohr magneton and the Landé coefficients corresponding, and $m_F = \pm 1$ is the magnetic quantum number of the respective states. All the atoms are assumed to be optically pumped to the states $|1\rangle$ and $|3\rangle$, which therefore have the same incoherent populations equal to $1/2$, i.e. $\rho_{11} = \rho_{33} = 1/2$ [19, 38]. The probe and control fields are directed towards a quarter-wave plate (QWP) to produce right- and left-circularly polarization components before interacting with the atoms [19, 38, 39]. Thus, the amplitude and phase difference of the two polarization electric field components can be varied by the QWP. Therefore, the Rabi frequencies have form $\Omega_p = \mu_{21}E_p/2\hbar = \Omega_{0p}(\cos\phi - \sin\phi)e^{-i\phi}$, and $\Omega_c = \mu_{23}E_p/2\hbar = \Omega_{0c}(\cos\phi + \sin\phi)e^{i\phi}$, where, ϕ is the rotated angle between the two polarization components. The denoted $\Delta_c = \omega_{23} - \omega_c$ and $\Delta_p = \omega_{21} - \omega_p$ are the frequency detuning of the coupling and probe fields, respectively. Following the electric dipole approximation and the rotating wave approximations, the interaction Hamiltonian of the system can be given by ($\hbar = 1$) [19, 38]:

$$H_{\text{int}} = (\Delta_p + \Delta_B)|2\rangle\langle 2| + (\Delta_p - \Delta_c + 2\Delta_B)|3\rangle\langle 3| - (\Omega_p|2\rangle\langle 1| + \Omega_c|3\rangle\langle 2| + H.c.) \quad (1)$$

The Liouville equation describes the dynamic evolution of the system:

$$\frac{\partial \rho}{\partial t} = -i[H_{\text{int}}, \rho] + \Lambda\rho, \quad (2)$$

and the relevant density matrix equations obtained for this system are given as follow [38]:

$$\dot{\rho}_{11} = \gamma_{31}(\rho_{33} - \rho_{11}) + \gamma_{21}\rho_{22} + i\Omega_p\rho_{21} - i\Omega_p\rho_{12}, \quad (3a)$$

$$\dot{\rho}_{22} = -(\gamma_{21} + \gamma_{23})\rho_{22} - i\Omega_p\rho_{21} + i\Omega_p\rho_{12} - i\Omega_c\rho_{23} + i\Omega_c\rho_{32}, \quad (3b)$$

$$\dot{\rho}_{33} = -\gamma_{31}(\rho_{33} - \rho_{11}) - \gamma_{23}\rho_{22} + i\Omega_c^*\rho_{23} - i\Omega_c\rho_{32}, \quad (3c)$$

$$\dot{\rho}_{21} = -(\gamma + i(\Delta_p + \Delta_B))\rho_{21} - i\Omega_p(\rho_{22} - \rho_{11}) + i\Omega_c\rho_{31}, \quad (3d)$$

$$\dot{\rho}_{31} = (-\gamma_{31} + i(\Delta_c - \Delta_p - 2\Delta_B))\rho_{31} - i\Omega_p\rho_{32} + i\Omega_c^*\rho_{21}, \quad (3e)$$

$$\dot{\rho}_{23} = (-\gamma + i(\Delta_B - \Delta_c))\rho_{23} + i\Omega_c(\rho_{33} - \rho_{22}) + i\Omega_p\rho_{13}, \quad (3f)$$

where, $\rho_{11} + \rho_{22} + \rho_{33} = 1$; $\rho_{ij} = \rho_{ji}^*$, $\gamma = (\gamma_{21} + \gamma_{23} + \gamma_{31})/2$, and γ_{ij} is the decay rate between levels $|i\rangle$ and $|j\rangle$, respectively.

Now, we put the ensemble of N degenerate two-level atoms into a one-dimensional ring cavity, as shown in figure 1(b). For simplicity, mirrors 3 and 4 are assumed 100% reflectivity, whereas R and T (with $R + T = 1$) are the reflection and transmission coefficients of mirrors 1 and 2, respectively. Furthermore, here only the probe field E_p is propagated through

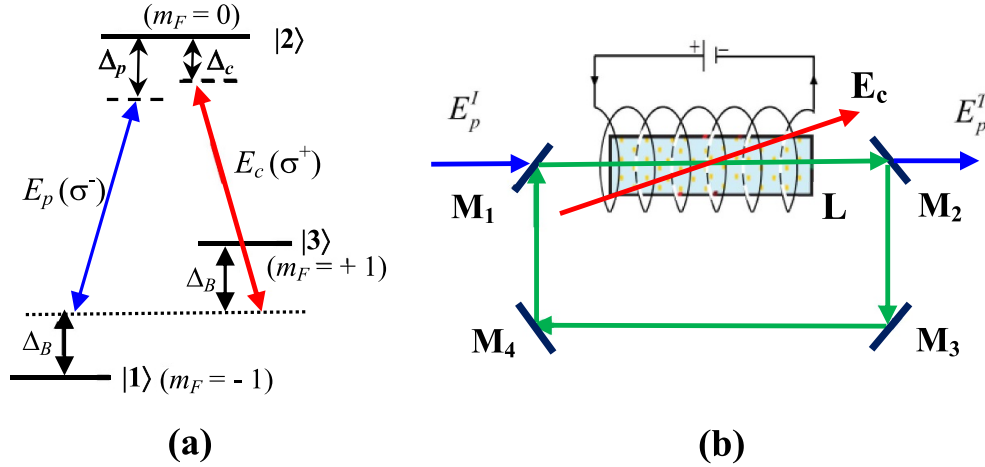


Figure 1. (a) The degenerate two-level atomic system under the interaction of coupling, probe, and external magnetic fields; (b) the unidirectional ring cavity contains an atomic sample of length L , E_p^I and E_p^T is the incident and transmission fields, respectively.

the cavity, whereas the coupling field E_c is not. The total electromagnetic field is represented by:

$$E = E_p e^{-i\omega_p t} + E_c e^{-i\omega_c t} + c.c., \quad (4)$$

Under the slowly varying envelope approximation, the probe field propagation is given by:

$$\frac{\partial E_p}{\partial t} + c \frac{\partial E_p}{\partial z} = i \frac{\omega_p}{2\varepsilon_0} P(\omega_p). \quad (5)$$

where $P(\omega_p)$ is induced polarization in transition $|1\rangle \leftrightarrow |2\rangle$:

$$P(\omega_p) = N\mu_{21}\rho_{21}. \quad (6)$$

From equations (5) and (6), we have:

$$\frac{\partial E_p}{\partial z} = i \frac{N\mu_{21}\omega_p}{2c\varepsilon_0} \rho_{21}. \quad (7)$$

With parameters of the perfectly tuned cavity and under the steady-state limit the boundary conditions between the input field E_p^I and the transmitted field E_p^T are as [38]:

$$E_p(L) = E_p^T/\sqrt{T}, \quad E_p(0) = \sqrt{T}E_p^I + RE_p(L). \quad (8)$$

The reflection mechanism of mirror M2 causes the bistability behavior, so if $R = 0$, there is no bistability. We can get the input-output relationship using equation (8) combining the mean-field limit and boundary conditions

$$y = x - iC\rho_{21}, \quad (9)$$

where $y = \mu_{21}E_p^I/\hbar\sqrt{T}$ and $x = \mu_{21}E_p^T/\hbar\sqrt{T}$ are the normalization of the fields, and $C = \frac{\omega_p N L |\mu_{21}|^2}{2\varepsilon_0 \hbar c T}$ is the cooperation parameter. The behavior of OB and OM under the influences of system parameters is considered in the following section by the numerical solving of equation (9) combined with equation (3) in the steady state, as displayed in figures 2–6.

3. Results and discussion

We apply the model for the cold ^{87}Rb atomic medium with the levels $|1\rangle$, $|3\rangle$, and $|2\rangle$ chosen corresponding to states: $5S_{1/2}$ ($F = 1$, $m_F = -1$), $5S_{1/2}$ ($F = 1$, $m_F = +1$), and $5P_{1/2}$ ($F = 1$, $m_F = 0$). The parameters are selected [19, 37]: $\gamma_{23} = \gamma_{21} = 2\pi \times 5.3$ MHz, $\gamma_{31} = 0.1\gamma_{21}$, $N = 4.5 \times 10^{17}$ atoms m^{-3} , $\mu_{21} = 1.6 \times 10^{-29}$ cm. The Landé and Bohr magneton coefficients are respectively: $g_F = -1/2$ and $\mu_B = 9.27401 \times 10^{-24}$ JT $^{-1}$. Here, the Zeeman shift Δ_B also calculated in units of γ_{21} , so the strength of the magnetic field B will be given in units of the combined constant $\gamma_c = \hbar\mu_B^{-1}g_F^{-1}\gamma_{21}$.

First, we analyze the influence of the coupling laser intensity Ω_c on the behavior of the OB for $\phi = \pi/6$ as shown in figure 2(a). Figure 2(a) shows that the threshold of OB initially significantly increases and then decreases although the coupling field continues to increase. Admittedly when the coupling laser field Ω_{0c} increases from $0.5\gamma_{21}$ to a value in the approach of $\Omega_{0c} = 2\gamma_{21}$, the OB threshold can reach the maximum value (dotted line in figure 2(a)) because the probe absorption reaches the saturation state, and at the same time multistability appears. However, the threshold of OB then decreases if we continue to increase Ω_c . Physically, as the strength of the coupling field increases, the probe absorption in the transition between states $|2\rangle$ and $|1\rangle$ dramatically reduces and the non-linearity of the medium is enhanced, which leads to a change in the behavior of the optical bistability. As a result, by controlling the coupling field intensity Ω_c , the threshold intensity of the OB can be manipulated. The effect of coupling laser field intensity on the OB for $\phi = 0$ is also shown in figure 2(b). In this case, it can be seen that the threshold intensity increases when the coupling field Ω_c is increasing and reaches a saturation value and then decreases gradually as Ω_c continues to rise [36, 38].

Next, the behavior of the OB under the influence of the magnetic field B for $\Delta_p = 0$ and $\Delta_p = 4\gamma_{21}$ at the $\phi = 0$ is displayed in figure 3. As designated in figure 3(a), the threshold intensity of OB first inflated significantly, and the OB curves

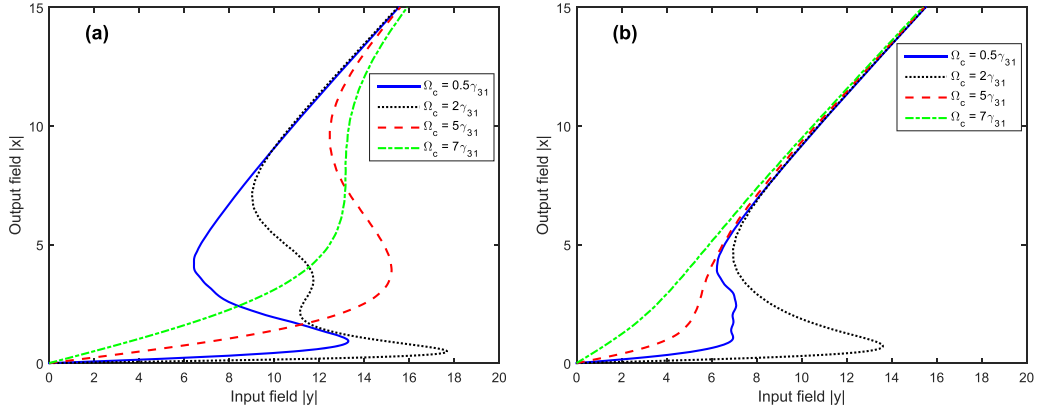


Figure 2. The bistability behavior at the different values of the coupling field Ω_c : for $\phi = \pi/6$ (a) and for $\phi = 0$ (b). The selected parameters are: $\Delta_c = \Delta_p = 0$, $C = 200$, $\Delta_B = 2\gamma_{21}$ or $B = 2\gamma_c$ and $\gamma_{23} = \gamma_{21}$, respectively.

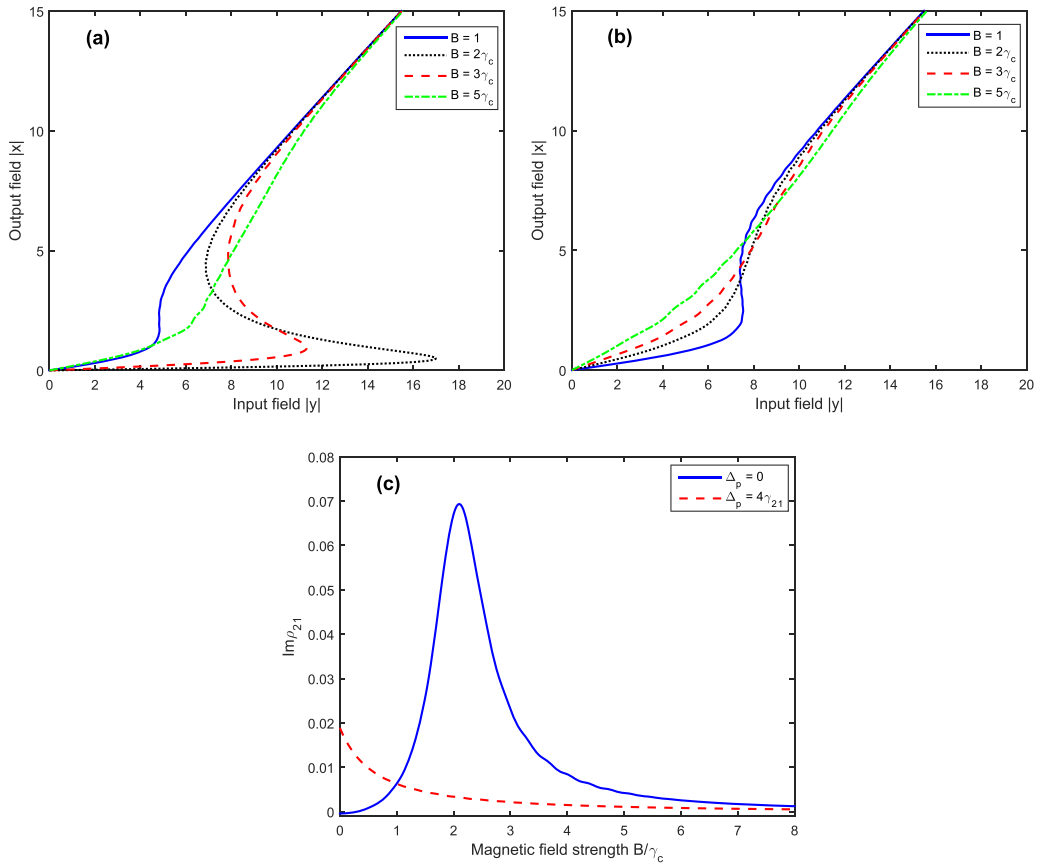


Figure 3. The bistability behavior at the different values of the magnetic field B : $\Delta_p = 0$ (a) and $\Delta_p = 4\gamma_{21}$ (b). The variation of the probe absorption versus magnetic field strength (c). The selected parameters are: $\phi = 0$, $\Omega_c = 3\gamma_{21}$, $\Delta_c = 0$, $C = 200$, and $\gamma_{23} = \gamma_{21}$, respectively.

width became greater as the magnetic field B increased but then decreased gradually although the magnetic field B continued to increase. Physically, increasing the strength of the magnetic field B causes the Zeeman level separation between the levels $|1\rangle$ and $|3\rangle$ to increase. As a result, the quantum interference between the two displacement channels $|2\rangle \leftrightarrow |1\rangle$ and $|2\rangle \leftrightarrow |3\rangle$ is reduced, so the probe absorption at the line center increases [36–38]. This absorption behavior is demonstrated through the probe absorption spectrum variation versus the magnetic field [see the blue solid line in figure 3(c)]. It shows

that the magnitude of the probe absorption first increases rapidly from zero to a maximal value corresponding with the increase of the magnetic field intensity and then reaches the steady-state value when the magnetic field intensity continuously increases. The impact of magnetic field B on the behavior of OB for $\Delta_p = 4\gamma_{21}$ is also shown in figure 3(b). The threshold of OB decreases as the magnetic field B is enhanced. Physically, when the magnetic field is non-zero, the probe absorption is reduced due to the shifting of the EIT window [38]. As a result, the probe absorption decreases and trends to a

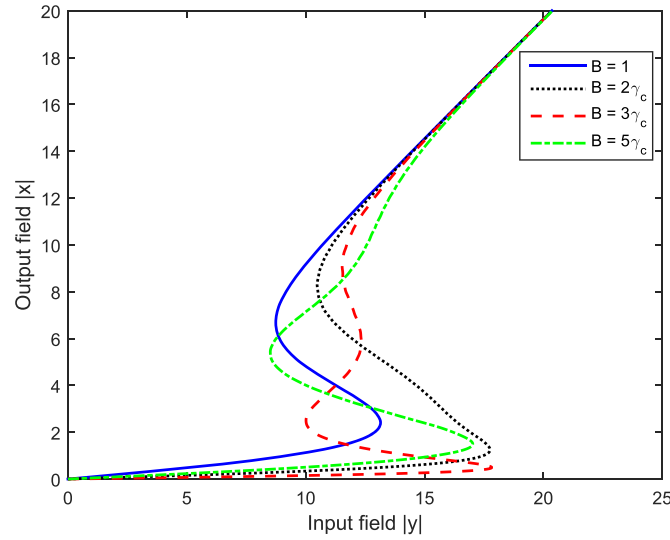


Figure 4. The bistability behavior at the different values of the magnetic field B for $\phi = \pi/6$. The selected parameters are: $\Omega_c = 3\gamma_{21}$, $\Delta_c = \Delta_p = 0$, $C = 200$, and $\gamma_{23} = \gamma_{21}$, respectively.

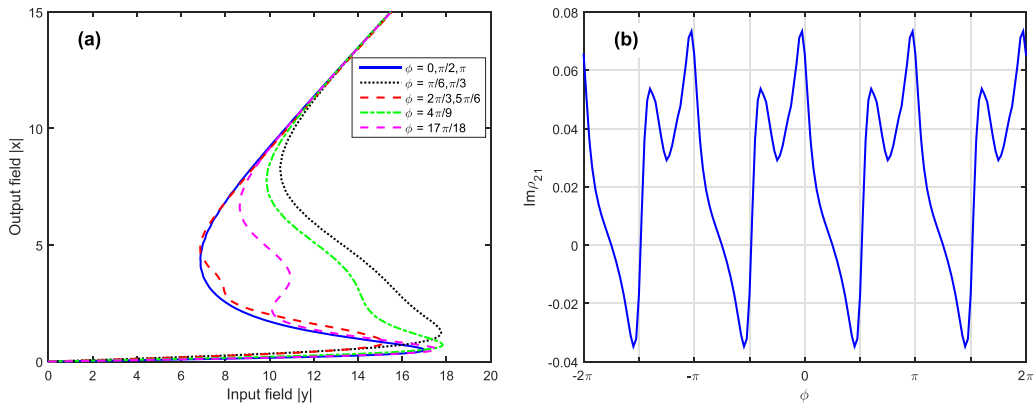


Figure 5. (a) The bistability behavior at the different values of the relative phase ϕ ; (b) The probe absorption as a function of the ϕ . The selected parameters are: $\Omega_c = 3\gamma_{21}$, $\Delta_B = 2\gamma_{21}$ or $B = 2\gamma_c$, $\Delta_p = \Delta_c = 0$ and $\gamma_{23} = \gamma_{21}$, respectively.

small steady-state value [see the red dashed line in figure 3(c)]. Thus, the threshold of OB is decreased and we barely obtain OB when magnetic field $B = 5\gamma_c$ or more extensive [the green dot–dash line in figure 3(b)]. Consequently, by adjusting the magnetic field B and the probe detuning to the proper value, the threshold and the width of the OB can be manipulated.

In figure 4, we present the shape of the OB curves for different values of the B when $\phi = \pi/6$. The result in figure 4 showed that we can convert from OB to OM (red dashed line) by changing the strength of the magnetic field B . The importance of this result leads to the practicality of multi-channel all-optical switching devices that are required for multiple outputs. Figure 5 displays the input-output relationship of the $|x|$ versus $|y|$ for different values of ϕ . It is shown that the behavior of the OB is changing versus relative phase ϕ because the probe absorption varies depending on the period versus the ϕ [36]. To clarify this, we plot the probe absorption versus the relative phase ϕ in figure 5(b). It can be seen that OM can appear at absorption peaks versus the relative phase. For example, at the $\phi = 17\pi/18$ (corresponding to the maximum

absorption peak in figure 5(b)), the OB converted to optical multistability. The appearance of the OM in these cases can be clarified by reconsidering the equation (8). The quantity y in equation (8) is not proportional to a cubic polynomial for variable x in the regions of investigated parameters. Therefore, the existence of OM depends on the optical characteristics of the atomic medium under the impact of the external magnetic field B and the relative phase ϕ . From the results obtained above, it is apparent that multistability in this model is possible only if the magnetic field B and the relative phase ϕ are co-existing. Thus, we can switch the OB to OM and vice versa by adopting proper magnetic field strength and the value of the polarization-dependent phase difference ϕ .

Finally, we present the dependence of the OB curves at the different values of the cooperation parameter C . From figure 6, it can be seen that the OB threshold is proportional to parameter C . This can be seen clearly in the relationship between parameter C and density N through an expression $C = \omega_p L |\mu_{21}|^2 N / 2\hbar \epsilon_0 c T$. Hence, the increase in parameter C goes along with increasing the atomic number density so that

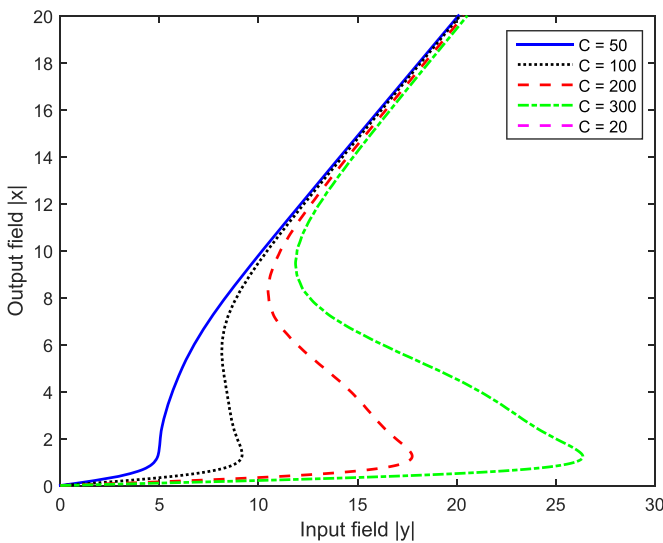


Figure 6. The bistability behaviors for different values of the parameter C . The selected parameters are: $\Omega_c = 3\gamma_{21}$, $\Delta_B = 2\gamma_{21}$ or $B = 2\gamma_c$, $\Delta_c = \Delta_p = 0$ and $\gamma_{23} = \gamma_{21}$, respectively.

the probe absorption will increase and increase the threshold of optical bistability.

4. Conclusion

In summary, we have realized OB and multistability in a degenerate two-level EIT medium under the impact of the outside magnetic field and the relative phase. By manipulating the strength of the magnetic field, we can change the threshold and width of the OB in different spectral domains of the probe field. Moreover, by changing the magnetic field intensity in the presence of the relative phase, OB can be easily converted to OM and vice versa. In addition, the effects of the control light intensity, the probe detuning, and the cooperation parameters on the properties of the OB also have been performed. The proposed model helps realize all-optical and optical-magnetic switches for applications in optical communications.

Acknowledgments

The study was supported by The Youth Incubator for Science and Technology Programme, managed by Youth Development Science and Technology Center-Ho Chi Minh Communist Youth Union and Department of Science and Technology of Ho Chi Minh City, the contract number is '01/2022/HĐ-KHCNT-VU'; Nga Luong Thi Yen was funded by the Postdoctoral Scholarship Programme of Vingroup Innovation Foundation (VINIF), code VINIF.2022.STS.52.

ORCID iD

Dong Hoang Minh  <https://orcid.org/0000-0003-0339-8192>

References

- [1] Joshi A and Xiao M 2012 *Controlling Steady-State and Dynamical Properties of Atomic Optical Bistability* (Singapore: World Scientific) (<https://doi.org/10.1142/7766>)
- [2] Gibbs H M, McCall S L and Venkatesan T N C 1976 Differential gain and bistability using a sodium-filled fabry-perot interferometer *Phys. Rev. Lett.* **36** 1135
- [3] Rosenberger A T, Orozco L A and Kimble H J 1983 Observation of absorptive bistability with two-level atoms in a ring cavity *Phys. Rev. A* **28** 2569
- [4] Fleischhauer M, Imamoglu A and Marangos J P 2005 Electromagnetically induced transparency: optics in coherent media *Rev. Mod. Phys.* **77** 633
- [5] Boller K J, Imamoglu A and Harris S E 1991 Observation of electromagnetically induced transparency *Phys. Rev. Lett.* **66** 2593
- [6] Harris S E 1997 Electromagnetically induced transparency *Phys. Today* **50** 36
- [7] Zibrov A S, Lukin M D, Nikonov D E, Hollberg L, Scully M O, Velichansky V L and Robinson H G 1995 Experimental demonstration of laser oscillation without population inversion via quantum interference in Rb *Phys. Rev. Lett.* **75** 1499–502
- [8] Schmidt H and Imamoglu A 1996 Giant Kerr nonlinearities obtained by electromagnetically induced transparency *Opt. Lett.* **21** 1936
- [9] Zhu C J, Hang C and Huang G X 2010 Gain-assisted giant Kerr nonlinearity in a Λ -type system with two-folded lower levels *Eur. Phys. J. D* **56** 231
- [10] Dong H M, Anh N T and Thanh T D 2022 Controllable Kerr nonlinearity in a degenerate V-type inhomogeneously broadening atomic medium aided by a magnetic field *Opt. Quant. Electron.* **54** 225
- [11] Hamed H R, Gharamaleki A H and Sahrai M 2016 Colossal Kerr nonlinearity based on electromagnetically induced transparency in a five-level double-ladder atomic system *Appl. Opt.* **22** 5892
- [12] Hau L V, Harris S E, Dutton Z and Bejroozi C H 1999 Light speed reduction to 17 m per second in an ultracold atomic gas *Nature* **397** 594–8
- [13] Thanh T D, Anh N T, Hien N T T, Dong H M, Hao N X, Khoa D X and Bang N H 2021 Subluminal and superluminal light pulse propagation under an external magnetic field in a vee-type three-level atomic medium *Photonics Lett. Pol.* **13** 4–6
- [14] Dong H M, Doai L V, Sau V N, Khoa D X and Bang N H 2016 Propagation of laser pulse in a three-level cascade atomic medium under conditions of electromagnetically induced transparency *Photonics Lett. Pol.* **8** 73
- [15] Khoa D X, Dong H M, Doai L V and Bang N H 2017 Propagation of laser pulse in a three-level cascade inhomogeneously broadened medium under electromagnetically induced transparency conditions *Optik* **131** 497
- [16] Dong H M, Doai L V and Bang N H 2018 Pulse propagation in an atomic medium under spontaneously generated coherence, incoherent pumping, and relative laser phase *Opt. Commun.* **426** 553
- [17] Dong H M, Nga L T Y, Khoa D X and Bang N H 2020 Controllable ultraslow optical solitons in a degenerated two-level atomic medium under EIT assisted by a magnetic field *Sci. Rep.* **10** 15298
- [18] Hamed H R 2017 Optical switching, bistability and pulse propagation in five-level quantum schemes *Laser Phys.* **27** 066002

- [19] Li J, Yu R, Si L and Yang X 2010 Propagation of twin light pulses under magneto-optical switching operations in a four-level inverted-Y atomic medium *J. Phys. B: At. Mol. Opt. Phys.* **43** 065502
- [20] Jafarzadeh H 2017 All-optical switching in an open V-type atomic system *Laser Phys.* **27** 025204
- [21] Dong H M and Bang N H 2019 Controllable optical switching in a closed-loop three-level lambda system *Phys. Scr.* **94** 115510
- [22] Anh N T, Thanh T D, Bang N H and Dong H M 2021 Microwave assisted all-optical switching in a four-level atomic system *Pramana J. Phys.* **95** 37
- [23] Khoa D X, Ai N V, Dong H M, Doai L V and Bang N H 2022 All-optical switching in a medium of a four-level vee-cascade atomic medium *Opt. Quant. Electron.* **54** 164
- [24] Brown A, Joshi A and Xiao M 2003 Controlled steady-state switching in optical bistability *Appl. Phys. Lett.* **83** 1301
- [25] Sheng J, Khadka U and Xiao M 2012 Realization of all-optical multistate switching in an atomic coherent medium *Phys. Rev. Lett.* **109** 223906
- [26] Harshwardhan W and Agarwal G S 1996 Controlling optical bistability using electromagnetic-field-induced transparency and quantum interferences *Phys. Rev. A* **53** 1812
- [27] Gong S, Du S and Xu Z 1997 Optical bistability via atomic coherence *J. Phys. Lett. A* **226** 293–7
- [28] Joshi A, Brown A, Wang H and Xiao M 2003 Controlling optical bistability in a three-level atomic system *J. Phys. Rev. A* **67** 041801(R)
- [29] Joshi A and Xiao M 2010 Atomic optical bistability in two- and three-level systems: perspectives and prospects *J. Mod. Opt.* **57** 1196–220
- [30] Abdelaziz A H M and Sarma A K 2020 Effective control and switching of optical multistability in a three-level V-type atomic system *Phys. Rev. A* **102** 043719
- [31] Gong S, Du S, Xu Z and Pan S 1996 Optical bistability via a phase fluctuation effect of the control field *J. Phys. Lett. A* **222** 237–40
- [32] Joshi A, Yang W and Xiao M 2003 Effect of quantum interference on optical bistability in the three-level V-type atomic system *J. Phys. Rev. A* **68** 015806
- [33] Cheng D, Liu C and Gong S 2004 Optical bistability and multistability via the effect of spontaneously generated coherence in a three-level ladder-type atomic system *J. Phys. Lett. A* **332** 244–9
- [34] Jafarzadeh H, Sahrai M and Ghaleh K 2014 Controlling the optical bistability in a Λ -type atomic system via incoherent pump field *Appl. Phys. B* **117** 927–33
- [35] Haifeng X 2019 Optical bistability and multistability via both coherent and incoherent fields in a three-level system *Laser Phys.* **29** 015205
- [36] Zhang D, Yu R, Li J, Ding C and Yang X 2013 Laser-polarization-dependent and magnetically controlled optical bistability in diamond nitrogen-vacancy centers *Phys. Lett. A* **377** 2621
- [37] Asadpour H and Soleimani H R 2014 Polarization dependence of optical bistability in the presence of external magnetic field *Opt. Commun.* **310** 120
- [38] Dong H M, Nga L T Y and Bang N H 2019 Optical switching and bistability in a degenerated two-level atomic medium under an external magnetic field *Appl. Opt.* **58** 4192–1499
- [39] Steck D A 2019 ⁸⁷Rb D line data (available at: <http://steck.us/alkalidata>)